



## Scaling effects on the ignition process in a single-side expansion scramjet combustor

Peiyi Li<sup>1</sup>, Zun Cai<sup>2</sup>, Yanan Wang<sup>3</sup>, Quanqi Wang<sup>3</sup>, Taiyu Wang<sup>3</sup>, Hongbo Wang<sup>3</sup>, Mingbo Sun<sup>3</sup>

### Abstract

Scramjet is developing from small scale to larger scale, it is an inevitable requirement to design large-scale engine based on the guidance of small-scale engine, according to the law of scaling effect. However, the researches on the scaling effect are mainly focused on the steady process of the supersonic flow and combustion, little attention has been paid to the unsteady process, such as ignition. In order to investigate the scaling effects on the unsteady process, the ignition process in the scramjet combustor of two different scales are studied by three-dimensional numerical simulations in this study. The k-omega SST two-equation turbulence model are used, and ignition process is modeled into the energy equation as an energy deposition term coupled with the finite rate model. Furthermore, by applying the energy deposition ignition model, detailed influence parameters affecting the ignition process, such as ignition energy and time, are comprehensively discussed. It is verified that there exists an obvious scaling effect in the ignition process, in addition, it is necessary to enlarge the ignition energy proportionally in the cavity-based combustor with different scales. As for the ignition process in the same combustor, it is found that the larger the ignition energy is, the faster the chemical reaction and initial flame propagation will be. However, at the same ignition energy, the influence of ignition power as well as time is neglectable on the ignition process.

**Keywords:** *Scaling effect, Ignition, Scramjet*

### Nomenclature (Tahoma 11 pt, bold)

A – Pre-exponential factor  
L – Length of cavity  
D<sub>1</sub> – Depth of cavity leading edge  
D<sub>2</sub> – Depth of cavity trailing edge  
P<sub>cavity</sub> – Dimensionless factor  
 $\dot{Q}$  – Energy source term  
T<sub>a</sub> – Activation energy  
T<sub>max</sub> – Maximum temperature  
a – Factor

b – Reaction order  
t<sub>0</sub> – time of maximum ignition power  
 $\alpha$  – Expansion angle  
 $\theta$  – Trailing edge inclination  
 $\varepsilon_i$  – Ignition energy  
 $\Delta_s$  – Characteristic scale  
 $\Delta_t$  – duration  
 $\sigma_s$  – and size parameter  
 $\sigma_t$  – duration parameter

### 1. Introduction

The scramjet engine is a potential propulsion system of air-breathing hypersonic vehicles, which has the highly military and economic value<sup>[1-3]</sup>. In the actual design process of scramjet engine, it is an inevitable requirement to design large-scale engine based on the guidance of small-scale engine. When

<sup>1</sup> Hypersonic Technology Laboratory National, University of Defense Technology, Changsha China, buaapeggy@163.com

<sup>2</sup> Hypersonic Technology Laboratory, National University of Defense Technology, Changsha China, caizun1666@163.com

<sup>3</sup> Hypersonic Technology Laboratory, National University of Defense Technology, Changsha China

the scramjet is enlarged or reduced geometrically, different characteristics of the flow and combustion are often appeared. In recent years, the scale effects of the scramjet are getting more and more attention.

Many researchers have studied the steady flow structure with combustion in the scramjet. Diskin and Northam<sup>[4]</sup> systematically studied the scale effects of the flow and the combustion in scramjet. The scale effects are attributed to the thickness of boundary layer and the nonlinearity of transverse jet. They studied the effects of multi-row nozzles, isolation length and equal area cavity length on the combustion field. Pulsonetti et al<sup>[5]</sup> summarized the scaling relationships of the ignition, the reaction, the boundary layer, and the mixing of hydrogen scramjet combustor. They designed experiments to study that the ignition time and the increase of the wall pressure follow the pressure length scaling criterion. Karl et al<sup>[6]</sup> studied the combustion scale effects by experimental and numerical means to verify whether different operating conditions conform to the pressure length scaling criterion of "PL= constant". Trebs et al<sup>[7]</sup> studied the effects of different scales of the inlet on supersonic combustion. Li Fan et al<sup>[8]</sup> carried out the experiments of kerosene combustion on two inflow scales with the air flow rate of 1.8kg/s and 3.6kg/s, respectively. They found that there is a scale effect in the flame stabilization mode. Li Zhen et al<sup>[9]</sup> found that the scale effects of the flame stabilization mode also exist in the axisymmetric scramjets. Ma Wenjie et al<sup>[10]</sup> constructed the scale magnification criterion equation and analyzed the approximate criterion by calculating the flame stability criterion number of the combustion chamber in the fuel-lean and fuel-rich combustion. The results showed that the flame rich blowout limit can be kept by adjusting the length-depth ratio of the cavity. Curran et al<sup>[11]</sup> studied the scale effects of accelerating scramjet by numerical simulation. They found that the thicker boundary layer and higher heat release in large-scale engine will lead to better combustion performance of large-scale engine.

Unsteady processes such as ignition are affected by flow and reaction. The nonlinear changes of reaction may affect the transient ignition process and the flame propagation, especially the mixing-dominated supersonic diffusion combustion flame. Li Liang et al<sup>[12]</sup> carried out a two-dimensional simulation study of combustion instability in the supersonic combustor with different scales to explore the influence of boundary layer thickness and fuel mixing efficiency on the combustion instability. It is found that the influence is mainly appeared in the recirculation region, and the decrease of the recirculation region will limit the flashback phenomenon. Zhao Guoyan et al<sup>[13]</sup> studied the scale effects of flame flashback in the ethylene-fueled scramjet with different scales, and found that the larger engine can obtain higher fuel mixing efficiency. As a result, the combustion is stronger and the flame flashback speed is faster.

The problem of effective start-up of scramjet requires reliable ignition. Up to now, the scale effect of ignition in the supersonic combustor has not been studied. Based on the three-dimensional numerical simulation, this paper studies the ignition process of scramjet combustor at different geometrical scales, and explores the effects of different ignition energy and time on the ignition process. The study will help to improve the understanding of scale effects on the ignition process in the scramjet.

## 2. Simulation setup

### 2.1. Calculation area

The numerical simulation adopts the high performance computing system of National Defense University of Science and Technology, and the parameters of supersonic inflow in this paper are cited from the experiment of the supersonic combustion<sup>[14]</sup>.

The computational domain also refer to the combustor in the experiment<sup>[14]</sup>. The combustor is a rectangular section with the width of 50 mm, the height of 40 mm and the length of 692mm, as seen in Fig 1. The ethylene injector is located on the upon side of the combustor, 10mm upstream the cavity, and on the spanwise central-line of the combustor. The diameter of the nozzle is 2.0mm. The cavity is located 355 mm downstream of the entrance. The trailing edge inclination  $\theta = 45^\circ$ , the depth of leading edge of cavity  $D_1 = 15$  mm, the depth of trailing edge  $D_2 = 12$ mm, the length of cavity  $L = 72$  mm, and the expansion angle  $\alpha = 2.25^\circ$ . Referring to the research<sup>[8]</sup>, all the physical geometrical length of the double-scale combustor are  $\sqrt{2}$  times longer than the reference one. It results in a 2 times mass flow rate at the inlet of the combustor. The calculation domain is shown in Fig 2.

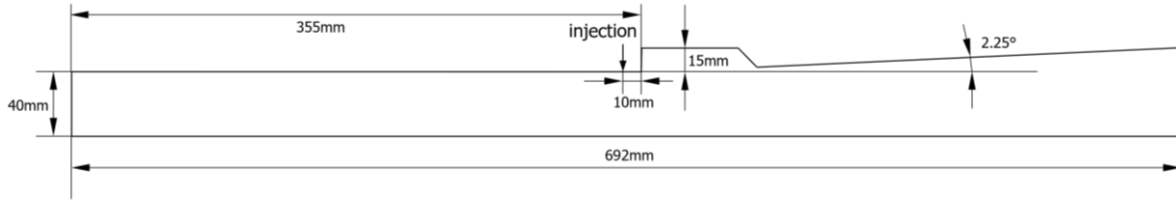


**Fig 1.** Sketch of the combustor models

The coordinate system adopts the right-handed coordinate system. The positive direction of the X axis is the direction of supersonic air flow, the positive direction of the Y axis points to the wall with cavity, and the positive direction of the Z axis adopts the right-handed system.

The three-dimensional model is used in this numerical simulation, and its calculation domain is shown in Fig 2.

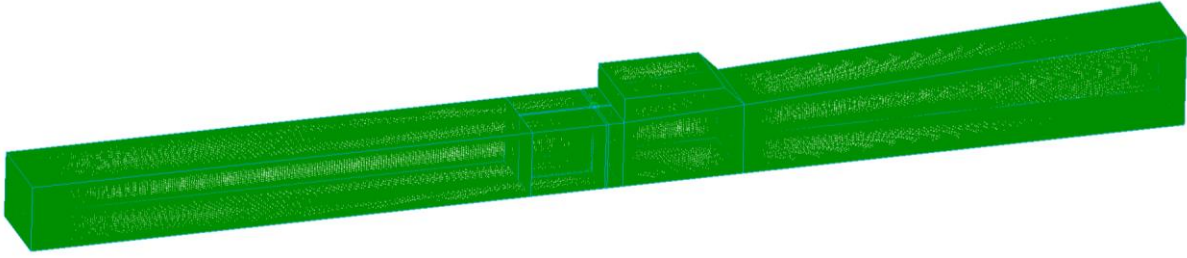


**Fig 2.** Calculation domain in this study

## 2.2. Numerical simulation method

### 2.2.1 Governing equations

This numerical simulation is mainly based on Reynolds average Navier-Stokes (RANS) method. The mass equation, momentum equation, energy equation and component transport of the compressible NS equation are as follows:

$$\frac{\partial \rho}{\partial t} + \frac{\partial(\rho u_j)}{\partial x_j} = 0 \quad (1)$$

$$\frac{\partial(\rho u_i)}{\partial t} + \frac{\partial(\rho u_i u_j + p \delta_{ij})}{\partial x_j} = \frac{1}{Re} \frac{\partial \tau_{ij}}{\partial x_j} \quad (2)$$

$$\frac{\partial E}{\partial t} + \frac{\partial[(E+p)u_j]}{\partial x_j} = \frac{1}{Re} \frac{\partial(q_j + u_i \tau_{ij})}{\partial x_j} \quad (3)$$

$$\frac{\partial \rho Y_i}{\partial t} + \nabla \cdot (\rho u Y_i - \rho D \nabla Y_i) = \rho \omega_i \quad (4)$$

Where  $\tau_{ij}$  is a viscous flux. According to the convention of Favre average (mass weighted average), the physical quantity of each item in the equation is decomposed, and then the time average of each item of the equation is taken, and the governing equation in RANS Reynolds average form can be obtained.

### 2.2.2 Chemical mechanism

In this paper, the laminar finite chemical reaction rate model is mainly used, and the chemical reaction rate is determined by Arrhenius formula. A simplified ethylene-air seven-component three-step chemical reaction mechanism is used. The mechanism of the reaction is simplified as shown in the Table 1.

**Table 1.** Seven-component three-step ethylene-air chemical reaction mechanism<sup>[15]</sup>

Reaction	$A/(\text{cm}^3 \cdot \text{mol}^{-1} \cdot \text{s}^{-1})$	$b$	$T_a/K$
$\text{C}_2\text{H}_4 + \text{O}_2 \leftrightarrow 2\text{CO} + 2\text{H}_2$	$2.100 \times 10^{14}$	0.0	18015.3
$2\text{CO} + \text{O}_2 \leftrightarrow 2\text{CO}_2$	$3.450 \times 10^{11}$	2.0	10134.9
$2\text{H}_2 + \text{O}_2 \leftrightarrow 2\text{H}_2\text{O}$	$3.000 \times 10^{20}$	-1.0	0

Where A is the pre-exponential factor of Arrhenius equation, b is the reaction order, and  $T_a$  is the activation energy divided by the molar gas constant.

The 2nd order Runge-Kutta scheme is used as the time scheme, and the upwind vector flux splitting scheme (AUSM-UP) is used as the space scheme.

### 2.3. Ignition model

To study the scale effect of the ignition process, we need to unify the simulation of the ignition process, firstly. During the simulation, the existing ignition mode of specifying ignition range and ignition temperature is not conducive to the exploration of ignition dynamic process and scale law, so it is necessary to establish an ignition model which is more suitable for the actual ignition energy excitation process.

Energy deposition (ED) ignition model<sup>[16]</sup> describes the energy brought by the ignition as a source term added to the energy equation to calculate the formation process of the initial fire core. This method significantly simplifies the physical process of the fire core formation. Though it cannot simulate plasma thermodynamics, it can certainly show the dependence of the ignition on the mixing. The ED model provides the real ignition energy distribution below the ionization temperature for the ignition process, as shown in Fig 3. This model has been used in direct numerical simulation (DNS) and large eddy simulation (LES) to study the early fire core formation and propagation of combustion flame<sup>[16]</sup>.

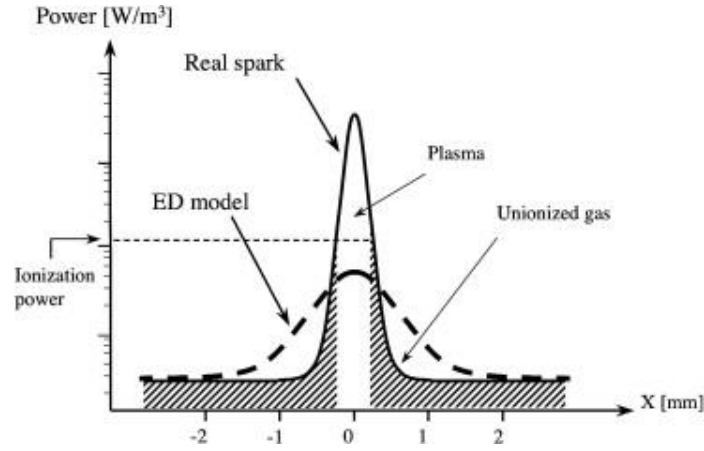


**Fig 3.** Sketch of power distributions for a real spark and for the ED model<sup>[16]</sup>

The source term added to the energy equation is described by three parameters: the ignition energy  $\varepsilon_i$  transferred to the gas, the duration  $\Delta_t$  and the characteristic scale  $\Delta_s$ .  $\dot{Q}$  is a source term related to position and time, which is then added to the energy equation with a Gaussian distribution in both time and space:

$$\dot{Q}(x, y, z, t) = \frac{\varepsilon_i}{4\pi^2 \sigma_s^3 \sigma_t} e^{-\frac{1}{2}(\frac{r}{\sigma_s})^2} e^{-\frac{1}{2}(\frac{t-t_0}{\sigma_t})^2} \quad (5)$$

Where  $r$  is the distance to the spark center,  $t_0$  is the time when the ignition power density reaches its maximum, and  $\sigma_s$  and  $\sigma_t$  are the parameters that control the size and duration of  $\dot{Q}$ :

$$\sigma_s = \frac{\Delta_s}{a} \quad (6)$$

$$\sigma_t = \frac{\Delta_t}{a} \quad (7)$$

Among them, the factor  $a = 4\sqrt{\ln(10)}$  enables 98% of the deposition energy in the range of " $\Delta_s^3 \times \Delta_t$ ". Without any heat loss, the characteristic scale " $\Delta_s$ " is such that the maximum temperature at the center of the fire core does not exceed a fixed temperature  $T_{max}$ .

For laser ignition, about 90% of the ignition energy will be lost in the shock wave and radiation effect, while for electric spark ignition, 70% to 90% of the energy will be lost in electrode heat conduction, radiation and shock wave expansion<sup>[16]</sup>. So the ignition energy transferred to the gas is about 10% of the total laser ignition energy or 10-30% of the total spark energy.

This ignition model transforms the ignition variables in the simulation from the abstract ignition range and ignition temperature to the ignition position and time which are closer to the actual application scene, which is more suitable for the study of scale effect in the ignition process. The ignition positions of all examples in this paper are located in the middle of the cavity, considering the energy loss caused

by the ignition position located on the wall of the cavity, the  $\alpha$  value in this study is half of the original value.

### 2.4. Grid independence validation

In order to limit the calculation error caused by the grid quantity, the grid independence verification is carried out. Three kinds of grids of 2 million, 7 million and 14 million are designed. The grid distribution is shown in Table 2, and the simulation is carried out under the same conditions.

**Table 2.** Mesh division accuracy

Grid Magnitude	Minimum Boundary layer Thickness/mm	Grid for Nozzles
2,000,000	0.02	84
7,000,000	0.01	160
14,000,000	0.007	253

The cold flow simulation results of three different grid sizes are shown in Fig 4 and Fig 5 below. As shown in the figure, the computational flow field of 2 million grid is relatively fuzzy compared with two outer large grid examples, especially the pressure of the flow passing through the shock is quite different from that of the other two kinds of the grids. Compared with 2 million grid and 14 million grid, the computational flow field of 7 million grid has been relatively clear, has a better simulation effect, and the grid size is not too large to bring pressure on the amount of calculation, so the benchmark example uses 7 million grid for calculation. Thus, the double-scale example doubles the grid to 14 million.

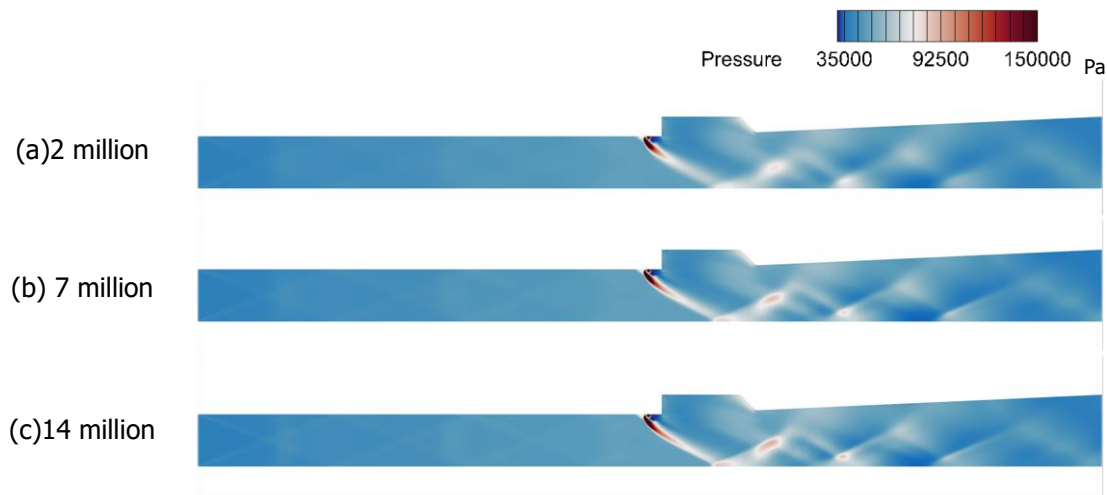


**Fig 4.** Static pressure contour of cold flow field of three different grid sizes

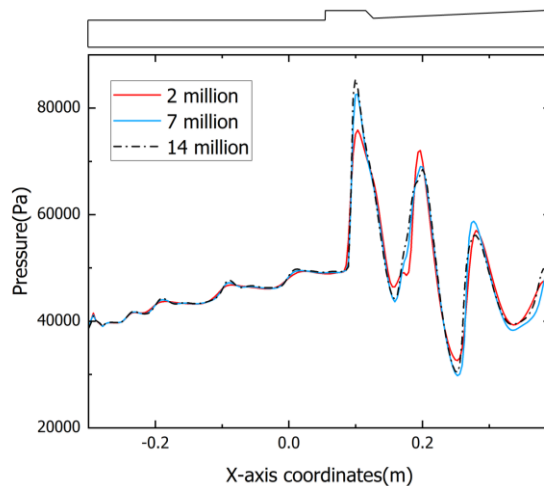


**Fig 5.** Wall pressure distribution on the bottom wall of the combustor

### 3. Results & Discussion

#### 3.1. Ignition energy

This section mainly explores the influence of ignition energy and combustor size growth on the ignition process. The differences on the scale and ignition energy are shown in Table 3.

**Table 3.** Ignition numerical setups of case 1-4

Case	Combustor Scale	Ignition Energy/J	Ignition Time
Case 1	1	0.5	0.01ms
Case 2	2	0.5	0.01ms
Case 3	2	1	0.01ms
Case 4	2	2	0.01ms

The volume of gas with more than 3% mass fraction of CO<sub>2</sub> in the three-dimensional space is extracted as the characterization of the flame mass in the combustor, which is projected onto the z plane of the cavity, and the ignition processes of different scale engines under different ignition energy conditions are compared in Fig 6.

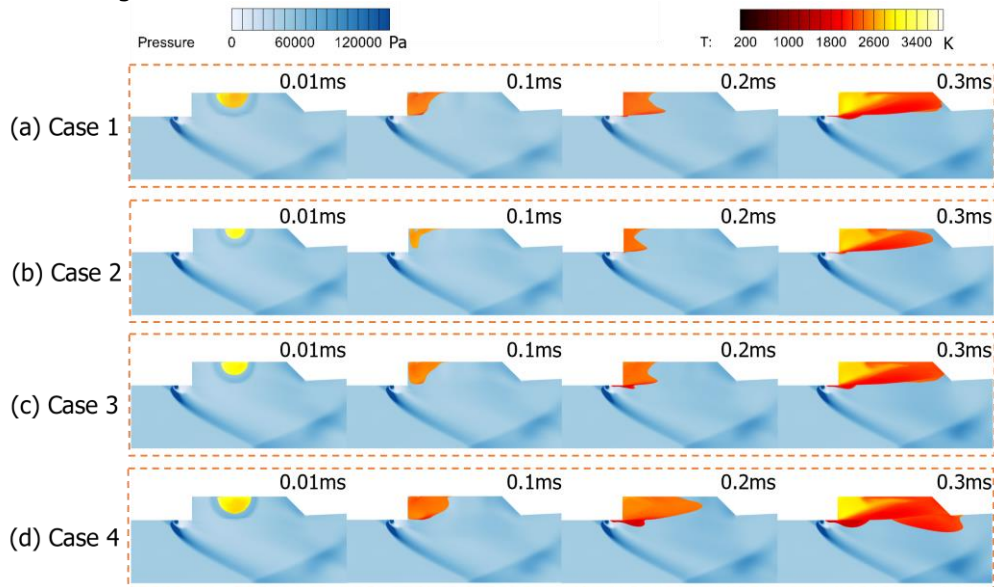


**Fig 6.** Static pressure and local temperature contours of ignition processes under different ignition energy

Comparing the ignition process in the combustor with different scale under the same ignition energy, it can be seen that the large-scale engine takes longer time to complete the ignition process under the same ignition energy. With the increase of ignition energy, the speed of the process from the initial flame core to flame stabilization is gradually accelerated.

To make this process more intuitive, the x coordinates of the farthest point from the front side of the gas with a mass fraction of more than 3% CO<sub>2</sub> in the cavity are extracted and dimensionless under different working conditions develops behind the cavity:

$$P_{cavity} = \frac{x_{3\%CO_2}}{L} \quad (10)$$

Where L is the total length of the cavity, the variation of this dimensionless parameter  $P_{cavity}$  with time under four different working conditions is compared as shown in Fig 7.



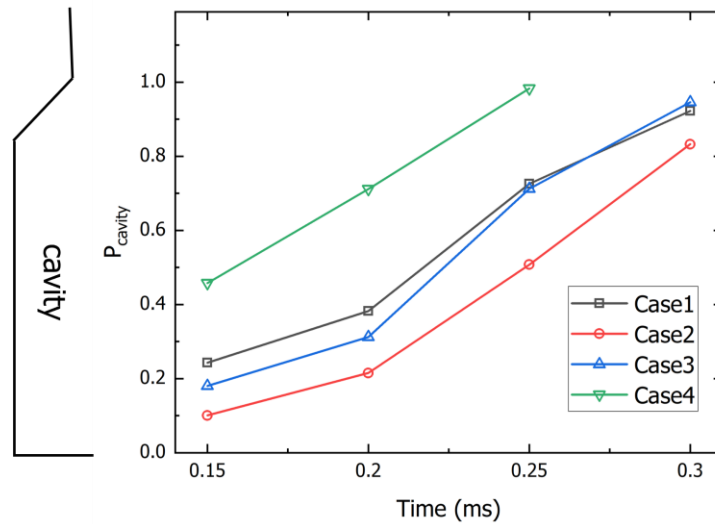


**Fig 7.** Comparison of dimensionless flame propagation distance inside the cavity

As shown in the Fig 7, the flame propagation process of Case 3 is more similar to that of Case1 in the cavity. Before 0.25ms, the flame propagation process of Case1 is slightly faster than Case3, and after 0.25ms, Case3 is faster than Case1. The time for the flame to fill the whole cavity is very similar. Compare the three-dimensional diagram of the flame development process of the two conditions, such as seen in Fig 8.

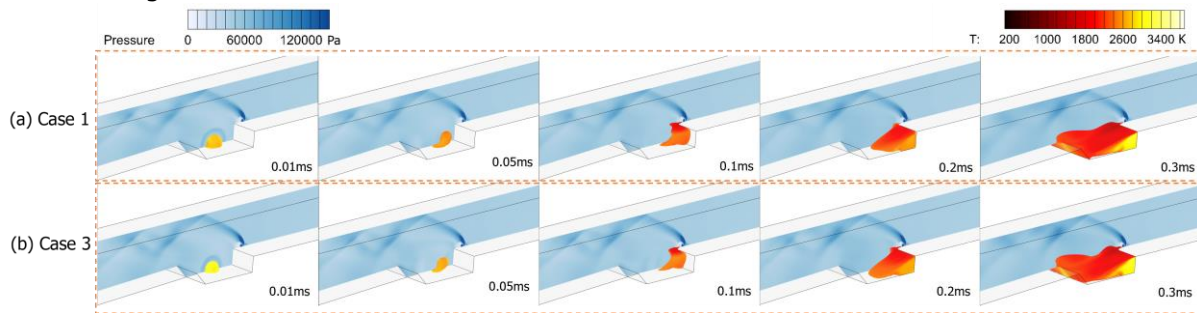


**Fig 8.** Static pressure and local temperature contours of flame propagation processes of case 1 and case 3

From the whole, the ignition process of the two-scale engine is very similar under the two specified operating conditions. Compared with the small-scale combustor, although the higher ignition energy brings higher ignition temperature, because of the consistent instantaneous range of ignition and the larger combustion chamber space, the relative initial development speed of flame in large-scale combustor is slightly slower than that in small-scale combustor. However, in the process of flame development from forward to backward in the cavity chamber, the flame growth and propagation speed is faster than that in the small-scale combustor. It is speculated that the reason for this phenomenon is that the large-scale combustor has better mixing.

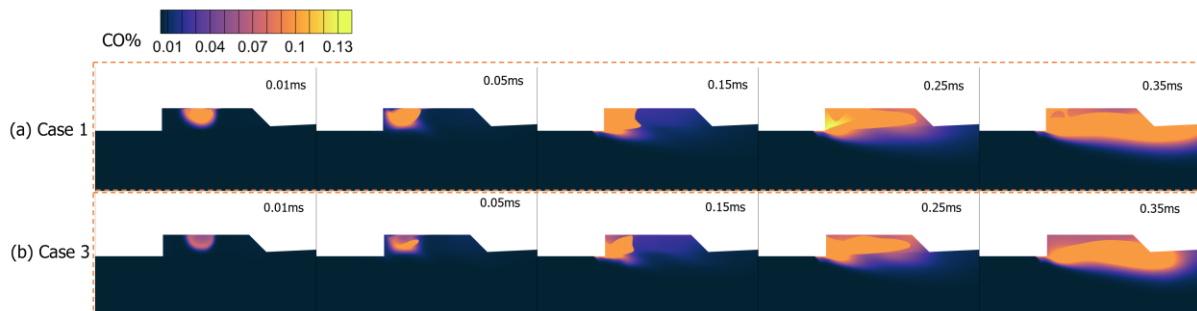


**Fig 9.** CO mass fraction contour and iso-surfaces of CO%=0.1 of case1 and case3

The changes of the combustion intermediate product CO of Case 1 and Case 3 during ignition were compared, and the iso-surface of  $\text{CO}\%=0.1$  was projected to the central cross section of the combustion chamber as shown in Fig 9. Compared with the distribution of combustion intermediates, the CO formation of Case 1 was significantly higher than that of case3 at the initial of ignition, which was different from that of Fig 8. It is speculated that the higher ignition energy and better mixing of Case 3 make the chemical reaction rate significantly higher than that of Case 1, so that less gas stays in the intermediate state of combustion.

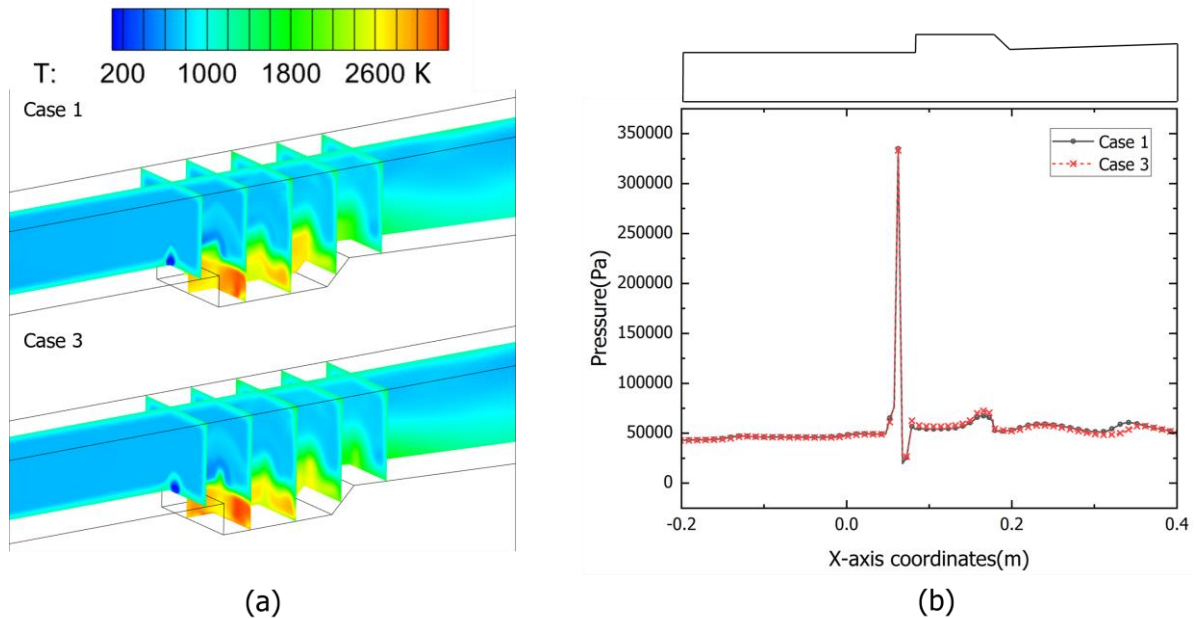


**Fig 10.** Comparison of Case 1 and Case 3 at 0.35ms:

(a) Static temperature; (b) Wall pressure on the cavity-side wall of the combustor.

At the time of 0.35ms after ignition, the temperature counters of Case 1 and Case 3 were shown in Fig 10, which is compared with the wall pressure of the central section of the cavity (in which the x coordinate of Case 1 is multiplied by  $\sqrt{2}$ ), the temperature distribution is similar and the pressure curve is basically the same, so it can be inferred that twice the ignition energy is needed to achieve the same effect as the reference combustor in the double scale combustor.

In addition, the ignition processes of two-scale engine with different ignition energy were compared and observed in Fig 11. With the increase of ignition energy, the initial temperature of the ignition area grows higher, the volume of air with chemical reaction is larger, and the flame propagates backward to form flame faster.

It is well known that after ignition in the middle of the cavity, due to the reflux effect of the cavity, the initial fire core will first move to the upstream of the cavity, then to the downstream of the cavity, and finally lift in the shear layer to form a global flame. By observing the development trajectory of different ignition energy in the two-scale combustor at the initial of ignition, it can be found that there is no great difference in the forward propagation velocity of the flame under the three conditions, but the range of the air mass with chemical reaction is larger. Therefore, the backward development speed of the ignition nucleus increases with the increase of energy. It is speculated that the reason for this phenomenon is that the higher ignition energy triggers a faster chemical reaction.



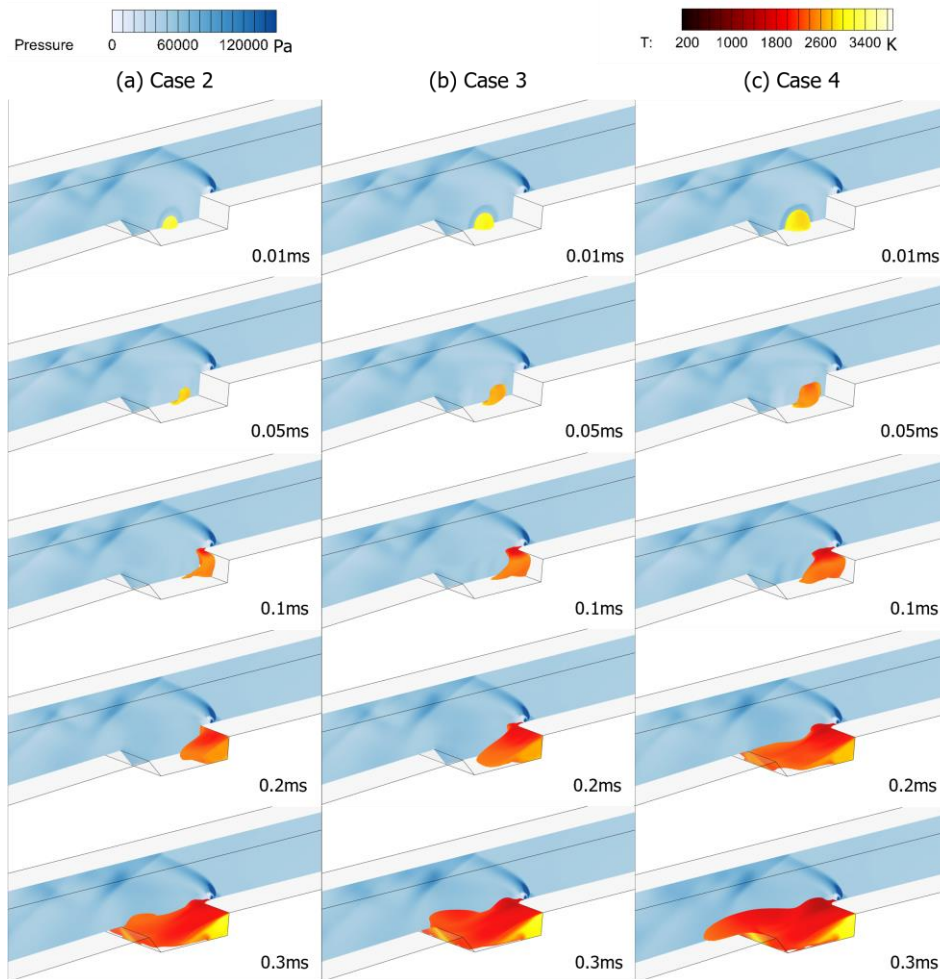


**Fig 11.** Static pressure and local temperature contours of of flame propagation processes of case 2-4

### 3.2. Ignition time

Larger combustor has longer residence time of the fire core and the ignition energy in the cavity, and prolonging the ignition time may affect the process. The main purpose of this section is to explore the influence of ignition time and combustion chamber size growth on the ignition process. The changes of scale and ignition time are shown in Table 4.

**Table 4.** Ignition numerical setups of case 1, 2, 5 and 6

Case	Combustor Scale	Ignition Energy/J	Ignition Time
Case 1	1	0.5	0.01ms
Case 2	2	1	0.01ms
Case 5	2	1	0.02ms
Case 6	2	1	0.04ms

The gas volume with more than 3% mass fraction of  $\text{CO}_2$  is extracted as the characterization of the flame cluster in the combustor, and the ignition processes of engines of different scales under different ignition time conditions are compared in Fig 12.

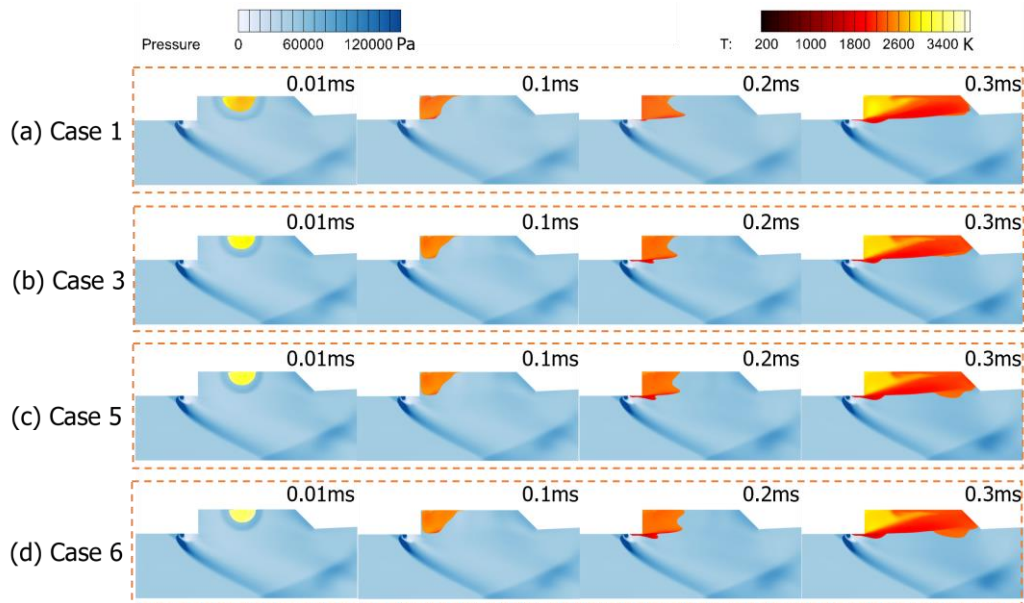


**Fig 12.** Static pressure and local temperature contours of ignition processes under different Ignition time:

By comparing and observing three cases with the same ignition energy and different ignition time under the same scale of combustor, it is found that the difference between different working conditions can not be judged only by observation, so the time variation of temperature volume integral of cavity within 0.05ms after ignition of Case3, Case5 and Case6 is further compared as shown in Fig 13.

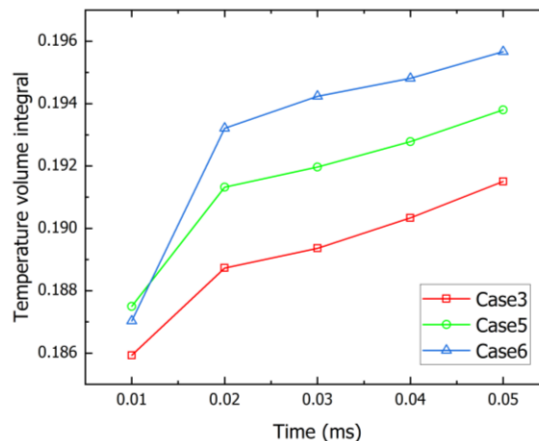


**Fig 13.** Comparison of temperature volume integral of the cavity with time at the initial stage of ignition.

Although the change is little, the increase of ignition time in the cavity did lead to more temperature increase. Longer ignition time made the temperature in the pre-0.02ms cavity rises faster. It is speculated that the continuous energy excitation can promote the chemical reaction to a certain extent, but because of the short duration and is in the early stage of the chemical reaction, the influence on the ignition process is limited. Under the condition of same total ignition energy, prolonging the ignition time has a little promoting effect on the ignition process, but it will not have much effect on the whole ignition process.

It is analyzed that the phenomenon may be related to the mathematical model used in the ignition model. In the energy deposition ignition model, the ignition energy decreases with time in the form of Gaussian distribution, the time setting prolongs the process of energy release. That means most of the energy is released in a relatively short time after ignition, and the flow field does not have enough influence on the change of the ignition process during this time. The energy given later accounts for too little in the total energy, so it is difficult to play an important role in the ignition process.

In the follow-up study, it can be considered to modify the mathematical model of ignition energy so that the amount of energy released remains unchanged within the specified duration of ignition, and then decreases along the Gaussian distribution with time, or the same energy is divided into several parts continuously released in a short time to simulate the extension of ignition time, to be carried out further research.

Due to the limited size, the ignition model used and working conditions of the combustion chamber studied in this study, the results had some limitations. In the future, more scales of combustors and more working conditions will be further studied, and different scales of combustor ignition experiments will be carried out in order to further explore the scaling effect law of the ignition process.

#### 4. Conclusion

Scaling effect is an important issue that must be solved for the scramjet application from laboratory to practical engineering. Aiming at the unsteady process of ignition in a scramjet, three-dimensional numerical simulations of combustors with different scales is carried out in this study. The existence of scaling effect during the ignition process is verified numerically. By comparing the ignition process with different ignition energy and ignition time, the influence of combustion chamber size on the ignition process is investigated. According to the simulation results achieved above, under the current simulation conditions, the characteristics of scaling effect during the ignition process is summarized as follows:

1. In the case of the same ignition time, in order to achieve the same ignition effect in the two-scale combustion chamber, it is necessary to enlarge the ignition energy proportionally;
2. In the same scale combustion chamber, the greater the ignition energy is, the faster chemical reaction and initial flame propagation is;
3. With equal total ignition energy, the effect of properly prolonging the ignition time on the ignition efficiency is neglectable.

#### Acknowledgements

This work was supported by the National Natural Science Foundation of China (Grant No. 12272408) and Natural Science Foundation for Distinguished Young Scholars of Hunan Province (2024JJ2057).

#### References

- [1] Huang W., Du Z., Yan L., Moradi R.: Flame propagation and stabilization in dual-mode scramjet combustors: a survey. *Progress in Aerospace Sciences*. 101, 13-30 (2018)
- [2] Wei J., Zhang S., Zuo J., Qin J., Zhang J., And, Bao W.: Effects of combustion on the near-wall turbulence and performance for supersonic hydrogen film cooling using large eddy simulation. School of Energy Science and Engineering, Harbin Institute of Technology, Harbin, Heilongjiang 150001, China. 35(3), 035112 (2023)
- [3] Chen E., Guo M., Tian Y., Zhang Y., Chen H., Le J., Zhong F., Zhang H.: Flame development prediction of supersonic combustion flow based on lightweight cascaded convolutional neural network. School of Energy Science and Engineering, Harbin Institute of Technology, Harbin, Heilongjiang 150001, China. 35(2), 1-17 (2023)
- [4] Diskin G. S., Northam G. B.: Effects of scale on supersonic combustor performance.(1987).
- [5] Pulsonetti M., Stalker R.: A study of scramjet scaling. *American Institute of Aeronautics and Astronautics*. [https://arc.aiaa.org/doi/10.2514/6.1996-4533\(1996\)](https://arc.aiaa.org/doi/10.2514/6.1996-4533(1996)).
- [6] Karl S., Hannemann K., Steelant J.: CFD Investigation of Scaling Laws for Hydrogen Fuelled Scramjet Combustors.(2008).
- [7] Trebs A., Roa M., Heister S., Anderson W., Lucht R.: Ramp Injector Scale Effects on Supersonic Combustion. *Journal of Propulsion and Power*. 30, 426-37 (2014)
- [8] Li F., Sun M., Zhu J., Cai Z., Wang H., Zhang Y., Sun Y.: Scaling effects on combustion modes in a single-side expansion kerosene-fueled scramjet combustor. *Chinese Journal of Aeronautics*. 34(5), 684-90. (2021)

- [9] 李桢, 顾洪斌. 不同尺度超燃燃烧室燃烧组织分析(Li Z.,Gu H.. Analysis of combustion structure of scramjet at different scales). proceedings of the The Fifth Joint Conference of Aerospace Propulsion (JCAP) and the 41st Technical Conference of Aerospace Propulsion Technology Information Society (APTIS). (2020).10.26914/c.cnkihy.2020.045039
- [10] Ma W., Shao W., Sun M., Wang Y., Wang Z., Xie S.: Scaling Effect of Supersonic Combustion Flame Stabilization Based on Driscoll Cavity Blowout Limits Model. Beijing Aerospace Technology Institute, Beijing, 100074, China;College of Aerospace Science and Engineering, National University of Defense Technology, Changsha, 410073, China. Vol.42(No.8), 1865 (2021)
- [11] Curran D., Wheatley V., Smart M.: High Mach Number Operation of Accelerator Scramjet Engine. University of Queensland, Brisbane, Queensland 4072, Australia\*PhD Candidate, Centre for Hypersonics, School of Mechanical and Mining Engineering University of Queensland, Brisbane, Queensland 4072, Australia†Associa. Vol.60(No.3), 884-98 (2023)
- [12] Li L., Liu M., Sun M., Tang T., Wang H., Zhao G.: Analysis of the Scale Effect of Supersonic Combustion Instability. Science and Technology on Scramjet Laboratory, College of Aerospace Science and Engineering, National University of Defense Technology, Changsha, 410073, China. Vol.27(No.4), 451 (2021)
- [13] Zhao G., Du J., Liu M., Wang H., Sun M.: Numerical investigation of the scale effects of the flame flashback phenomenon in scramjet combustors. Science and Technology on Scramjet Lab, National University of Defense Technology, Changsha, 410073, China. Vol.119(Part 2), 107165 (2021)
- [14] Ji J., Cai Z., Wang T., Wang Z., Sun M.: Experimental Study on Combustion Modes and Oscillations in a Cavity-Based Scramjet Combustor. AIAA Journal. 62(3), 915-27. (2024)
- [15] Brindle A., Boyce R., Neely A.: CFD Analysis of an Ethylene-Fueled Intake-Injection Shock-Induced-Combustion Scramjet Configuration.(2005).
- [16] Lacaze G., Richardson E., Poinot T.: Large eddy simulation of spark ignition in a turbulent methane jet. Combustion and Flame. 156(10), 1993-2009. (2009)